J Supercond Nov Magn (2009) 22: 337–342
DOI 10.1007/s10948-008-0440-y

LETTER

Muon-Spin Rotation Study of the Ternary Noncentrosymmetric Superconductors $Li_2Pd_xPt_{3-x}B$

P.S. Häfliger · R. Khasanov · R. Lortz · A. Petrović · K. Togano · C. Baines · B. Graneli · H. Keller

Received: 10 December 2008 / Accepted: 15 December 2008 / Published online: 13 January 2009

Abstract We investigated the superconducting state of the noncentrosymmetric superconductors $Li_2Pd_xPt_{3-x}B$ with superconducting transition temperature $T_c = 5.16(8)$ K ($x = 2.25$), 3.56(8) K ($x = 1.5$) and 2.60 K ($x = 0$) by means of muon-spin rotation (μSR) and specific heat experiments. The μSR relaxation rate σ_{sc} was found to be constant at low temperatures for all the compounds. Data taken at different magnetic fields show that the magnetic penetration depth λ is field-independent for $Li_2Pd_{2.25}Pt_{0.75}B$ and Li_2Pt_3B. The electronic contribution to the specific heat measured in $Li_2Pd_{1.5}Pt_{1.5}B$ and Li_2Pt_3B increases exponentially at the lowest temperatures. These features suggest that the *whole family* of $Li_2Pd_xPt_{3-x}B$ comprises single-gap s-wave superconductors across the entire doping regime.

Keywords Noncentrosymmetric superconductors · Magnetic penetration depth

P.S. Häfliger · B. Graneli · H. Keller
Physik-Institut der Universität Zürich, Winterthurerstrasse 190, 8057 Zürich, Switzerland

R. Khasanov (✉) · C. Baines
Laboratory for Muon-Spin Spectroscopy, Paul Scherrer Institute, CH-5232 Villigen PSI, Switzerland
e-mail: rustem.khasanov@psi.ch

R. Lortz · A. Petrović
Département de Physique de la Matière Condensée de Genève, 24 quai Ernest-Ansermet, 1211 Geneva, Switzerland

K. Togano
National Institute for Materials Science, 1-2-1 Sengen, Tsukuba 305-0047, Japan

1 Introduction

Superconductivity in systems without inversion symmetry has recently attracted considerable interest, see e.g. [1, 2]. The basic pairing states for a superconductor can be generally classified as spin-singlet and spin-triplet states. Cooper pairing in the spin-singlet channel is based on time-reversal symmetry (Anderson's theorem) [3], whereas for spin-triplet pairing also the existence of an inversion center in the crystal lattice is necessary [4]. However, the lack of an inversion center in the crystal lattice induces an antisymmetric spin–orbit coupling (ASOC) which is not destructive to special spin-triplet states as has been shown by Frigeri et al. [5] in the case of $CePt_3Si$, for instance.

Lately the noncentrosymmetric superconductors Li_2Pd_3B and Li_2Pt_3B have been discovered [6–9]. This system presents an ideal playing field to study superconductivity without inversion symmetry since there is no sign of magnetic order or strong electron correlation effects [6] such as was found in $CePt_3Si$, for instance. A significant effort was put into identifying the superconducting state using various experimental methods. While measurements of the penetration depth [10] and nuclear magnetic resonance (NMR) experiments [11] suggest the existence of spin-triplet states and nodes in the gap of Li_2Pt_3B, specific heat data indicate conventional behavior as expected for an isotropic single-gap *s*-wave superconductor in Li_2Pd_3B and Li_2Pt_3B compounds [7]. Furthermore, our previous muon-spin rotation (μSR) and magnetization experiments on Li_2Pd_3B show no sign of an unconventional superconducting pairing state [12, 13].

In order to shed light on this controversy, we have performed a systematic study of $Li_2Pd_xPt_{3-x}B$ at different doping levels x choosing the bulk-sensitive transverse-field

muon-spin rotation (TF-μSR) technique. Therewith we investigated the temperature and field dependence of the μSR relaxation rate σ in $Li_2Pd_xPt_{3-x}B$ with $x = 2.25$, 1.5 and 0. In addition, we measured the low-temperature specific heat of $Li_2Pd_{1.5}Pt_{1.5}B$ and Li_2Pt_3B.

2 Experiments

$Li_2Pd_xPt_{3-x}B$ was prepared by two-step arc-melting [6] for various doping concentrations. Details of the sample preparation can be found elsewhere [12]. The field-cooled magnetization of all the compounds was measured using a superconducting quantum interference device (SQUID) magnetometer in fields ranging from 0.5 mT to 1.6 T at temperatures between 1.75 and 10 K. Specific heat was measured from 6 down to 0.1 K.

TF-μSR experiments were performed at the πM3 beam line at the Paul Scherrer Institute, Villigen, Switzerland. The $Li_2Pd_xPt_{3-x}B$ ($x = 2.25$, 1.5 and 0) samples were field-cooled from above T_c down to 30 mK in fields of 0.1, 0.02 and 0.01 T. We performed temperature scans at low fields for all the samples. Field-dependent data up to 1.5 T were taken for $Li_2Pd_{2.25}Pt_{0.75}B$ and Li_2Pt_3B where each point includes a set of data at $T > T_c$ and at 1 K after cooling in the field.

The μSR signal was recorded in the usual time-differential way by counting positrons from decaying muons as a function of time. The field distribution $P(B)$ is then obtained from the Fourier transform of the measured time spectra $P(t)$. $P(t)$ is fitted with a Gaussian line and an oscillatory term for the signal originating from the sample as well as for the signal belonging to the sample holder (silver plate). Figure 1 illustrates the $P(t)$ and $P(B)$ distributions inside the Li_2Pt_3B sample in the mixed state at 0.05 K after being field-cooled in a magnetic field of 0.01 T. The second moment of $P(B)$ is related to the μSR relaxation rate σ which contains the superconducting component σ_{sc} as well as a contribution from the nuclear moments, $\sigma^2 = \sigma_{sc}^2 + \sigma_n^2$.

3 Results and Discussion

In extreme type-II superconductors such as Li_2Pd_3B (Ginzburg–Landau parameter $\kappa \approx 27$ [12]), the magnetic field distribution $P(B)$ is almost independent of the coherence length ξ [14]. The magnetic penetration depth λ can then be calculated from the known value of σ_{sc} using Brandt's formula describing the field variation in an ideal triangular vortex lattice [15]:

$$\sigma_{sc}\ [\mathrm{m\,s^{-1}}] = 4.83 \times 10^4 (1-h)\left[1 + 1.21\left(1-\sqrt{h}\right)^3\right]\lambda^{-2}\ [\mathrm{nm}] \quad (1)$$

where $h = H/H_{c2}$, with H_{c2} the upper critical field. Details can be found elsewhere, see e.g. [12].

The magnetic field dependence of the second moment of $\sigma_{sc}(1\ \mathrm{K})$ for $Li_2Pd_{2.25}Pt_{0.75}B$ and Li_2Pt_3B is displayed in the middle and right panels of Fig. 2, respectively. For the sake of completeness we also show the field dependence of $\sigma_{sc}(0)$ for Li_2Pd_3B [12] in the left panel. The data are taken at a fixed field at a temperature $T > T_c$, the sample is then field-cooled to 1 K in order to determine σ_{sc} and σ_n unambiguously for each field. The insets illustrate the corresponding temperature dependence of the upper critical field H_{c2} as obtained from magnetization (Li_2Pd_3B and $Li_2Pd_{2.25}Pt_{0.75}B$) and specific heat measurements (Li_2Pt_3B). Clearly $H_{c2}(T)$ can be satisfactorily fitted with the model based on the Werthamer–Helfand–Hohenberg (WHH) theory [16], as demonstrated by the solid lines. The results for $H_{c2}(0)$ are listed in Table 1. H_{c2} is then inserted into (1) in order to fit $\sigma_{sc}(H)$ to the experimental data with λ as a fit parameter. The results are in excellent agreement with the experimental data (shown by solid lines) implying that λ is field-independent. The deviation at low fields ($h \leq 0.003$ in the case of $Li_2Pd_{2.25}Pt_{0.75}B$) is expected since (1) is no longer valid at this region. In the case of Li_2Pt_3B the error bars are large due to the

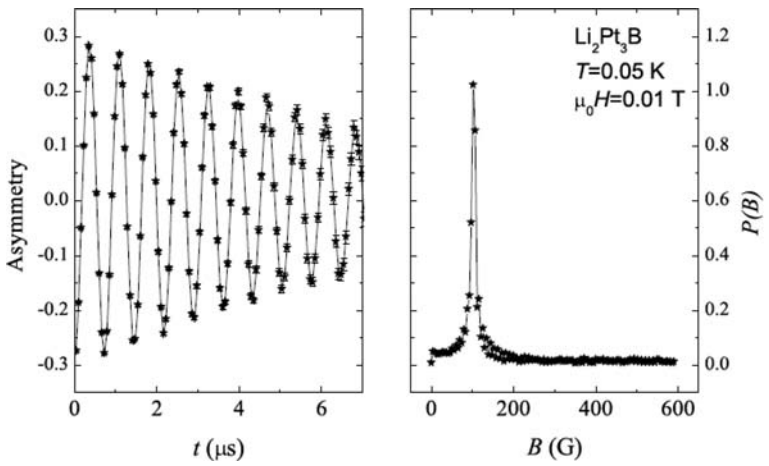

Fig. 1 μSR time spectrum (*left panel*) and magnetic field distribution (*right panel*) of Li_2Pt_3B taken in $\mu_0 H = 0.01$ T below the superconducting transition temperature $T_c = 2.60$ K (0.05 K). The lines represent a Gaussian fit as explained in the text

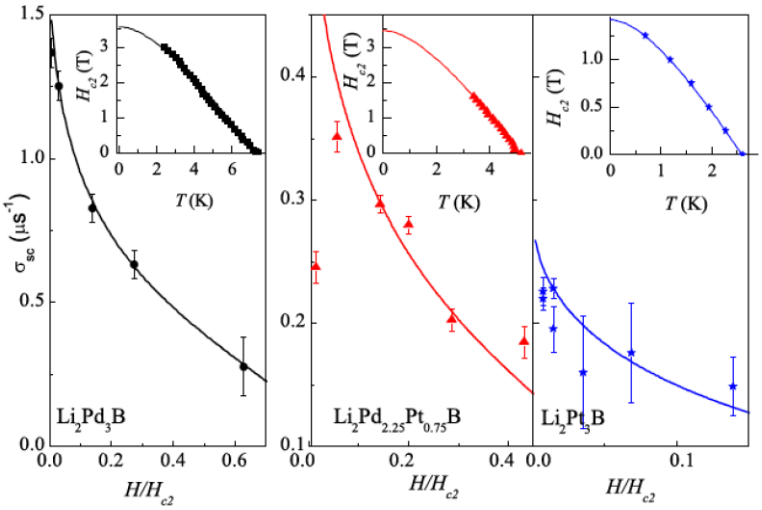

Fig. 2 Field dependence of the μSR depolarization rate $\sigma_{sc}(T = 1\ \mathrm{K})$ in $Li_2Pd_xPt_{3-x}B$ for $x = 3$ (*left panel*) [12] as well as $x = 2.25$ (*middle panel*) and 0 (*right panel*). The solid lines correspond to the results of a least-squares fitting procedure based on (1) as described in the text. In the *insets* the upper critical field H_{c2} vs. temperature T is shown with the *solid lines* corresponding to a fit based on the WHH model

Table 1 Summary of the normal state and superconducting parameters for $Li_2Pd_xPt_{3-x}B$ obtained in the present study from μSR measurements. The meaning of the parameters is explained in the text

x	T_c [K]	$\mu_0 H_{c2}$ [T]	$\lambda(0)$ [nm]	$\kappa(0)$	Δ_0 [meV]	$2\Delta_0/k_B T_c$
3	7.66(5)*a*	3.66(8)*a*	252(2)*a*	27(1)*a*	1.53(4)	4.4(2)
2.25	5.16(8)	3.35(9)	413(8)	42(1)	1.03(4)	4.4(3)
1.5	3.56(8)	2.27(8)	–	–	0.59(2)	3.7(2)
0	2.60(5)	1.42(6)	608(10)	40(1)	0.41(2)	3.4(3)

small value of the relaxation rate σ_{sc}. The resulting penetration depth $\lambda(1\ \mathrm{K})$ equals 413(8) nm and 608(10) nm for $Li_2Pd_{2.25}Pt_{0.75}B$ and Li_2Pt_3B, respectively, while we obtained $\lambda(0) = 252(2)$ nm for Li_2Pd_3B [12], see Table 1. The value of $\lambda(0)$ for Li_2Pd_3B is in agreement with magnetization measurements performed by Badica et al. [9], whereas our results for $\lambda(0)$ for $Li_2Pd_{2.25}Pt_{0.75}B$ and Li_2Pt_3B deviate from those in [9].

The superconducting coherence length ξ may be estimated from H_{c2} as $\xi = [\Phi_0/(2\pi H_{c2})]^{0.5}$. We obtain $\xi(0) = 9.5(2)$ nm (Li_2Pd_3B) [12], $\xi(1\ \mathrm{K}) = 9.9(2)$ nm ($Li_2Pd_{2.25}Pt_{0.75}B$) and 15.2(8) nm (Li_2Pt_3B). This results in a value for $\kappa(0) = \lambda(0)/\xi(0)$ of 27(1) for Li_2Pd_3B [12] with $\kappa(1\ \mathrm{K}) = 42(1)$ and 40(1) for $Li_2Pd_{2.25}Pt_{0.75}B$ and Li_2Pt_3B, respectively (see Table 1). Since λ is constant at low temperatures as will be shown later, we may set $\xi(0) \approx \xi(1\ \mathrm{K})$ as well as $\lambda(0) \approx \lambda(1\ \mathrm{K})$. The compounds in the present work are thus extreme type-II superconductors; μSR is therefore an appropriate tool for penetration depth studies.

We also measured the temperature dependence of the μSR signal in order to extract $\lambda^{-2}(T)$ using (1). The results are displayed in Fig. 3 for the entire doping series $Li_2Pd_xPt_{3-x}B$ ($x = 0$, 1.5, 2.25 and 3 [12]). The second moment of $P(B)$ increases with x, and $\lambda^{-2}(x)$ monotonically grows in turn with increasing Pd content. We observe that $\lambda^{-2}(T)$ saturates at low temperatures and becomes T-independent for all the compounds. This indicates that the Fermi surface is fully gapped down to the lowest temperatures. Thus we applied a model for a BCS s-wave superconductor in order to fit the data (see e.g. [17])

$$\frac{\lambda^{-2}(0)}{\lambda^{-2}(T)} = 1 + 2 \cdot \left\langle \int_0^\infty d\varepsilon \frac{df}{dE} \right\rangle. \tag{2}$$

Here $\langle \ldots \rangle$ represents an angular average over the Fermi surface, f is the Fermi function and $E = \sqrt{\varepsilon^2 + |\Delta|^2}$ the total energy with ε the single-particle energy measured from the Fermi surface. Since we have assumed an isotropic gap, i.e. s-wave symmetry, the superconducting gap Δ is k-independent, but only depends on temperature T such that $\Delta(T) = \Delta_0 \cdot \tanh(a\sqrt{T_c/T - 1})$ with $a = 1.74$ [18]. The resulting gap values at zero temperature Δ_0 are listed in Table 1. Over the whole temperature range (T_c down to 30 mK) and in the whole doping range ($0 \le x \le 3$) λ^{-2} is consistent with what is expected for an isotropic BCS superconductor. However, the BCS fit to the Li_2Pt_3B data is not satisfactory. In Li_2Pt_3B a considerable spin-triplet contribution has previously been observed in [10, 11], thus we assumed a mixture of spin-triplet states associated with a strong antisymmetric spin–orbit coupling resulting in two bands as presented in [10]. Assuming the same set of parameters and a BCS-temperature dependence of the superconducting gaps (black dotted line in Fig. 3d), $\lambda^{-2}(T)$ differs significantly from our results. If we assume that the gap with nodes is smeared out due to inhomogeneity of the sample, the resulting model calculations are in agreement with our experimental data, as illustrated by the solid black line in Fig. 3d. At this point we cannot exclude the existence of spin-triplet states.

In order to clarify matters, the superconducting state was also investigated by an independent study of the specific heat. Figure 4 illustrates the specific heat obtained for $Li_2Pd_{1.5}Pt_{1.5}B$ (left panel) and Li_2Pt_3B (right panel) in zero

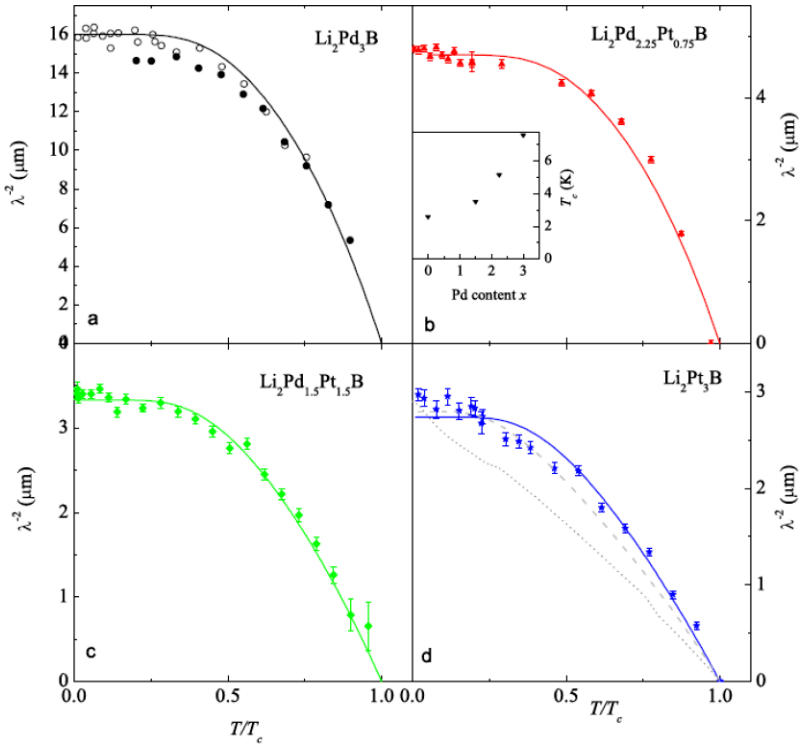

Fig. 3 Temperature dependence of λ^{-2} in $Li_2Pd_xPt_{3-x}B$ for $x = 3$ at 0.02 T (*black open circles*) and 0.5 T (*black solid circles*) (*panel* **a**), 2.25 (*panel* **b**), 1.5 (*panel* **c**) and 0 (*panel* **d**) at 0.01 T. The solid lines correspond to a least-squares fit to the experimental data for a BCS single-gap *s*-wave superconductor based on (2) with the parameters given in the text. In *panel d*, the *gray dashed* and *dotted lines* correspond to a model based on a two-gap scenario where one and both bands become superconducting, respectively; see text for explanation. The *inset* of *panel b* illustrates T_c as a function of Pd doping *x*

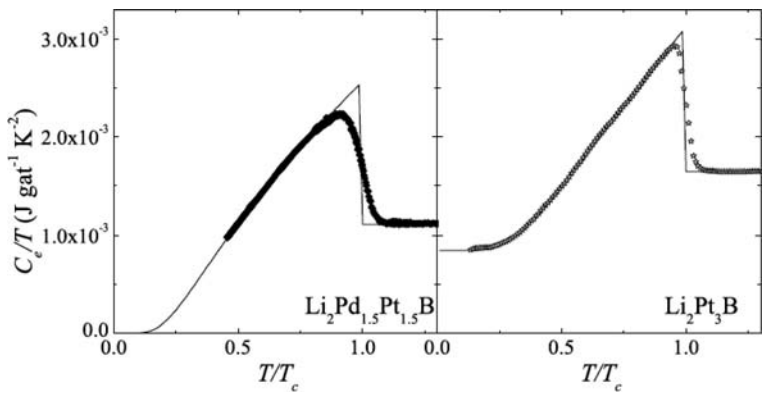

Fig. 4 Specific heat of $Li_2Pd_{1.5}Pt_{1.5}B$ (*left panel*) and Li_2Pt_3B (*right panel*)

Table 2 Summary of the normal state and superconducting parameters for $Li_2Pd_xPt_{3-x}B$ obtained in the present study from specific heat measurements. The meaning of the parameters is explained in the text

x	T_c [K]	$\mu_0 H_{c2}$ [T]	γ	$\Delta C/\gamma T_c$ [mJ/gat K^2]	Δ_0 [meV]	$2\Delta_0/k_B T_c$
3	7.66(5)*a*	3.66(8)*a*	1.50(2)*b*	2.0(3)*b*	1.30(4)*b*	3.94(4)*b*
2.25	5.16(8)	3.35(9)	–	–	–	–
1.5	3.56(8)	2.27(8)	1.10(2)	1.28(3)	0.37(2)	3.3(2)
0	2.60(5)	1.42(6)	1.66(2)	1.75(2)	0.45(2)	4.0(2)

field. The electronic contribution C_e/T to the specific heat of Li_2Pt_3B, as obtained in a standard procedure by quenching superconductivity in a field of 4 T, shows an exponential increase at the lowest temperature. This is consistent with our μSR data and therefore implies that Li_2Pt_3B is a fully gapped superconductor. A fit using a standard single-gap *s*-wave BCS model gives an excellent result (see Fig. 4). We obtain a gap-to-T_c ratio of $2\Delta_0/k_BT_c = 4.0(2)$ which is slightly larger than the μSR value but still in reasonable agreement. A smaller value of $2\Delta_0/k_BT_c = 3.3(2)$ is derived for $Li_2Pd_{1.5}Pt_{1.5}B$ (see Table 2). A particularity of Li_2Pt_3B is a rather large residual Sommerfeld coefficient γ_r. A possible explanation is that within a two-gap scenario as presented by Yuan et al. [10] only one gap becomes superconducting, while the gap with nodes is smeared out due to inhomogeneity of the sample. However, we have measured

another piece of the same large sample and we found a variation of γ_r of approximately 30%, but the superconducting contribution remains unchanged. This behavior is typical for macroscopic metallic inclusions which remain in the normal state. Details of the specific heat measurements will be published elsewhere.

Interestingly, results in the literature postulate several different superconducting ground states for the $Li_2Pd_xPt_{3-x}B$ family. In particular, previous work on Li_2Pt_3B deviates substantially from our conclusions. For instance, Yuan et al. [10] found a linear temperature dependence of the low-temperature penetration depth in Li_2Pt_3B by using a tunnel-diode based, self-inductive technique. The results were interpreted on the basis of a parity-mixed state with two Fermi surfaces induced by the lack of inversion symmetry coupled with a strong ASOC. The authors found that in Li_2Pt_3B one of the superconducting gaps changes sign due to the enhanced ASOC, which leads to line nodes in the superconducting gap and therefore explains the non-saturating penetration depth. None of our data—neither μSR nor specific heat—supports such a scenario. We believe that the difference in the experimental data arises from the different experimental techniques. In [10] data are taken by using a surface sensitive technique with the magnetic field only penetrating a distance λ below the surface (200–600 nm, see Table 1). Muons, on the other hand, penetrate to much bigger distances (fraction of millimeters) and therefore allow us to study the magnetic penetration depth in the bulk. The specific heat is also a bulk-sensitive technique. Bearing these in mind, the discrepancy between the results obtained in the present study and those reported in [10] can be explained by the difference between the bulk and the surface properties of $Li_2Pd_xPt_{3-x}B$, in analogy with what was observed in conventional [19] and unconventional [20] superconductors. We would also like to emphasize that our data are in excellent agreement with the specific heat data presented in [7]. Takeya et al. found values for $2\Delta_0/k_BT_c = 3.94(4)$ and 3.53 for Li_2Pd_3B and Li_2Pt_3B, respectively, which are in reasonable agreement with our results obtained from μSR measurements.

We will briefly comment on the results of Nishiyama et al. [11] obtained using the nuclear magnetic resonance (NMR) technique which is also bulk-sensitive. They deduce the existence of triplet states in Li_2Pt_3B from the Knight shift. However, it is not clear why they use a p-wave model to fit the data for the spin relaxation rate. Furthermore, they predict the behavior for an s-wave symmetry of the superconducting gap in Li_2Pt_3B by using the value for the superconducting gap of Li_2Pd_3B which is more than three times bigger, see Table 1. In addition, the absence of a Hebel–Slichter peak in the spin relaxation does not necessarily imply that the sample under investigation has an anisotropic gap.

4 Conclusions

In conclusion, we have performed muon-spin rotation, specific heat and magnetization measurements on the ternary boride superconductor $Li_2Pd_xPt_{3-x}B$. The main results are: (i) the field dependence of the μSR relaxation rate is consistent with Brandt's formula, (ii) the upper critical field H_{c2} obeys the WHH model, (iii) the temperature dependence of λ^{-2} and (iv) the specific heat data are consistent with what is expected for an s-wave BCS superconductor. The temperature dependence of λ^{-2} of Li_2Pt_3B can also be explained by the existence of two bands induced by an ASOC where only the one without nodes contributes to superconductivity due to inhomogeneity of the sample. But specific heat data indicate the existence of metallic inclusions. All our measurements and analysis strongly point to a single isotropic superconducting gap. No signature of an exotic superconducting order parameter was found. Thus we suggest that the *whole family* of $Li_2Pd_xPt_{3-x}B$ is a standard BCS superconductor with a single, isotropic gap.

Acknowledgements This work was partly performed at the Swiss Muon Source (SμS), Paul Scherrer Institute (PSI, Switzerland). We are grateful to N. Hayashi and M. Sigrist for helpful discussions as well as to H. Takeya for providing us the samples $Li_2Pd_xPt_{3-x}B$, $x = 3,\ 2.25,\ 1.5$ and 0. This work was supported by the Swiss National Science Foundation and the K. Alex Müller Foundation.

References

1. Hayashi, N., Wakabayashi, K., Frigeri, P.A., Sigrist, M.: Phys. Rev. B **73**, 024504 (2006)
2. Bauer, E., Hilscher, G., Michor, H., Paul, Ch., Scheidt, E.W., Gribanov, A., Seropegin, Yu., Nöel, H., Sigrist, M., Rogl, P.: Phys. Rev. Lett. **92**, 027003 (2004)
3. Anderson, P.W.: J. Phys. Chem. Solids **11**, 26 (1959)
4. Anderson, P.W.: Phys. Rev. B **30**, 4000 (1984)
5. Frigeri, P.A., Agterberg, D.F., Koga, A., Sigrist, M.: Phys. Rev. Lett. **92**, 097001 (2004)
6. Togano, K., Badica, P., Nakamori, Y., Orimo, S., Takeya, H., Hirata, K.: Phys. Rev. Lett. **93**, 247004 (2004)
7. Takeya, H., Hirata, K., Yamaura, K., Togano, K., El Massalami, M., Rapp, R., Chaves, F.A., Ouladdiaf, B.: Phys. Rev. B **72**, 104506 (2005)
8. Badica, P., Kondo, T., Kudo, T., Nakamori, Y., Orimo, S., Togano, K.: Appl. Phys. Lett. **85**, 4433 (2004)
9. Badica, P., Kondo, T., Togano, K.: J. Phys. Soc. Jpn. **74**, 1014 (2005)
10. Yuan, H.Q., Agterberg, D.F., Hayashi, N., Badica, P., Vaderwelde, D., Togano, K., Sigrist, M., Salamon, M.B.: Phys. Rev. Lett. **97**, 017006 (2006)
11. Nishiyama, M., Inada, Y., Zheng, G.-G.: Phys. Rev. Lett. **98**, 047002 (2007)
12. Khasanov, R., Landau, I.L., Baines, C., La Mattina, F., Maisuradze, A., Togano, K., Keller, H.: Phys. Rev. B **73**, 214528 (2006)
13. Landau, I.L., Khasanov, R., Togano, K., Keller, H.: Physica C **451**, 134 (2007)
14. Brandt, E.H.: Phys. Rev. B **37**, 2349 (1988)

15. Brandt, E.H.: Phys. Rev. B **68**, 054506 (2003)
16. Werthamer, N.R., Helfand, E., Hohenberg, P.C.: Phys. Rev. **147**, 295 (1966)
17. Kim, M.-S., Skinta, J.A., Lemberger, T.R., Kang, W.N., Kim, H.-J., Choi, E.-M., Lee, S.-I.: Phys. Rev. B **66**, 064511 (2002)
18. Bonalde, I., Yanoff, B.D., Salamon, M.B., Van Harlingen, D.J., Chia, E.M.E., Mao, Z.Q., Maeno, Y.: Phys. Rev. Lett. **85**, 4775 (2000)
19. Khasanov, R., Di Castro, D., Paderno, Yu., Filippov, V., Brütsch, R., Keller, H.: Phys. Rev. B **72**, 224509 (2005)
20. Khasanov, R., Shengelaya, A., Bussmann-Holder, A., Karpinski, J., Keller, H., Müller, K.A.: J. Supercond. Nov. Magn. **21**, 81 (2008)